JACS
JOURNAL OF THE AMERICAN CHEMICAL SOCIETY

ARTICLE

pubs.acs.org/JACS

Understanding the Role of the Sulfide Redox Couple (S^{2-}/S_n^{2-}) in Quantum Dot-Sensitized Solar Cells

Vidhya Chakrapani,[†,∥] David Baker,[†,‡] and Prashant V. Kamat*[,†,‡,§]

[†]Notre Dame Radiation Laboratory, [‡]Department of Chemical and Biomolecular Engineering, and [§]Department of Chemistry and Biochemistry, University of Notre Dame, Notre Dame, Indiana 46556, United States

Supporting Information

ABSTRACT: The presence of sulfide/polysulfide redox couple is crucial in achieving stability of metal chalcogenide (e.g., CdS and CdSe)-based quantum dot-sensitized solar cells (QDSC). However, the interfacial charge transfer processes play a pivotal role in dictating the net photoconversion efficiency. We present here kinetics of hole transfer, characterization of the intermediates involved in the hole oxidation of sulfide ion, and the back electron transfer between sulfide radical and electrons injected into TiO_2 nanoparticles. The kinetic rate constant (10^7-10^9 s^{-1}) for the hole transfer obtained from the emission lifetime measurements suggests slow hole scavenging from CdSe by S^{2-} is one of the limiting factors in attaining high overall efficiency. The presence of the oxidized couple, by addition of S or Se to the electrolyte, increases the photocurrent, but it also enhances the rate of back electron transfer.

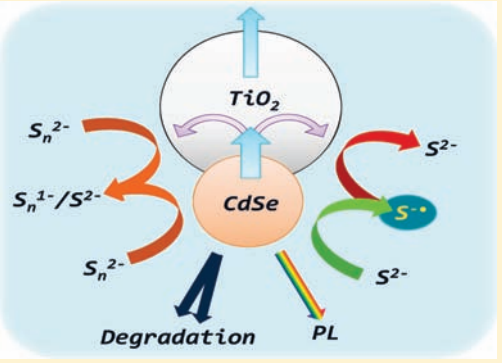

INTRODUCTION

Metal chalcogenides have played an important role in developing solar cells because of their response to visible light and their ability to deliver stable photocurrent.[1−5] Early efforts of using single crystal and polycrystalline metal chalcogenides (CdS and CdSe) in photoelectrochemical cells have provided a fundamental understanding of the energetics and interfacial charge transfer kinetics.[6−8] A crucial aspect in liquid junction solar cells is the interplay between hole transfer to the redox couple and hole-induced anodic corrosion.[9] Sulfide electrolytes are effective in scavenging the photogenerated holes and can tackle the issues related to anodic photocorrosion.[10,11] For example, the sulfide/polysulfide redox couple is effective in scavenging the holes of CdS and CdSe, but it cannot suppress anodic corrosion of the CdTe electrode.[10]

More recently, research interest in CdS- and CdSe-based liquid junction solar cells has been rejuvenated because of the emergence of quantum dots.[2,4,12−15] The ability to control optical and electrical properties of these semiconductor nanocrystals by means of size and shape provides the flexibility to tune the performance of solar cells. The sensitization of CdS or CdSe quantum dots on nanocrystalline metal−oxide surfaces (typically TiO_2) is achieved by SILAR, chemical bath deposition, electrochemical deposition, electrophoresis, and linker assisted binding.[16−24] Because of the porous geometry of the metal oxide film, more surface area is available for sensitization. This means the electrolyte is in much more intimate contact with the working electrode.

The redox couple plays an important role in the regeneration of the semiconductor by scavenging photogenerated holes.[2] To date, the sulfide/polysulfide redox couple has remained the popular redox couple that assists in delivering high open circuit voltage and stability of solar cell operation.[25−28] The role of sulfide/polysulfide couple in the operation of the QDSC, however, is yet to be fully understood. By employing SiO_2 and TiO_2 coated with 4 nm CdSe nanoparticles, we have probed the hole transfer at the working electrode/electrolyte interface. The photoelectrochemical and transient absorption experiments that elucidate the effects of S^{2-}/S_n^{2-} redox couple on the overall performance of QDSC are presented here (Scheme 1).

EXPERIMENTAL SECTION

Materials. Cadmium oxide (CdO, Aldrich), tetradecylphosphonic acid (TDPA, PCI Synthesis), trioctylphosphine oxide (TOPO, Aldrich), dodecylamine (DDA, Aldrich), selenium (Se, Aldrich), and trioctylphosphine (TOP, Aldrich) were used as received to prepare CdSe QDs. 3-Mercaptopropionic acid (3-MPA, Aldrich), P-25 TiO_2 powder (Evonik), and colloidal SiO_2 suspension (Nalco 2327) were used to prepare QD films. Fluorinated tin oxide (FTO) coated glass slides (Pilkington) were used as optically transparent electrodes.

Synthesis of CdSe QDs. CdSe QDs were prepared by the hot injection method with some modifications.[29] Briefly, CdO (0.39 mmol), TOPO (5.2 mmol), TDPA (1.1 mmol), and DDA (5.4 mmol) were degassed under vacuum at 110 °C for 1 h and then heated under nitrogen to 315 °C until the solution turned colorless. TOPSe (0.25 mmol of Se dissolved in 4.25 mL of TOP) was subsequently injected into the hot solution to initiate the nucleation. The heating was stopped when the nanoparticles grew to the desired size. After 2 min of growth at

Received: April 5, 2011
Published: May 13, 2011

dx.doi.org/10.1021/ja203131b | J. Am. Chem. Soc. 2011, 133, 9607–9615

Scheme 1. Demonstration of Possible Electron Pathways[a]

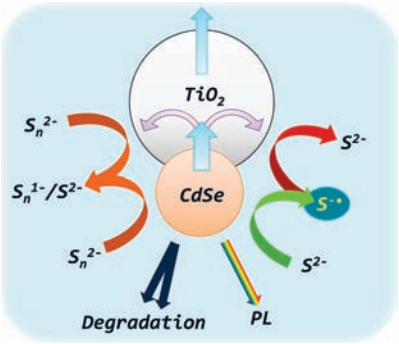

[a] Red and orange arrows show electron scavenging by the electrolyte, while the green arrow shows hole scavenging by S^{2-} to the intermediate $S^{-\bullet}$. Blue arrows are the desired electron transfer pathway through TiO_2 to the backing electrode. Degradation of the quantum dot and radiative recombination are other possibilities for the fate of the excited electron.

270 °C, the QD solution was cooled to room temperature, washed three times with a mixture of methanol and toluene, and suspended in toluene for use. Steady-state absorption measurements on as-synthesized quantum dots in toluene showed the typical $1S_{3/2}1S_e$ transition at 550 nm; see Figure S1 in the Supporting Information. By comparing this excitonic peak to the absorption curve reported by Peng and coworkers,[29] the particle diameter was estimated to be 3.9 nm.

Preparation of CdSe−TiO_2 Films. Opaque TiO_2 films were prepared for electrical and photoluminescence measurements using P25 TiO_2 powder. TiO_2 powder was mixed with a 1:4 (wt %) mixture of ethyl cellulose and terpeniol and then doctor bladed on an FTO slide. Transparent TiO_2 films for absorption measurements were prepared applying TiO_2 paste (Dyesol) onto glass slides with doctor blade method. The resulting films were typically 3 μm thick. All samples were annealed at 120 °C for 15 min prior to the final annealing at 400 °C for 1 h.

Preparation of CdSe−SiO_2 Films. Opaque SiO_2 films were prepared on FTO slides through direct spray coating. Colloidal SiO_2 nanoparticle suspension (Nalco 2327) was diluted with water (1:2) and sprayed onto FTO slide mounted on a hot plate. Repeated steps of spraying and air drying yielded an 8 μm film. Transparent SiO_2 films were prepared by spin coating SiO_2 suspension.

All films were subjected to a final 400 °C heat treatment for 2 h. Films were then cooled to 120 °C and were placed directly in a 1 M MPA in acetonitrile solution for 12 h. Films were washed with acetonitrile and then toluene, and placed directly in a CdSe quantum dot solution for 48 h.

Characterization. UV−vis absorption spectra of transparent CdSe−TiO_2 and CdSe−SiO_2 films were recorded using a Varian CARY 50 Bio UV−visible spectrophotometer in transmission mode. Absorption measurements on opaque films were performed in diffuse reflectance mode using a Shimadzu UV-3101 PC spectrophotometer. Steady-state emission spectra were recorded with a Jobin Yvon Fluorolog-3 spectrofluorometer. Fluorescence emission lifetime measurements were measured using a Horiba Jobin Yvon single photon counting system with a diode laser (373 nm, 250 kHz repetition, and 300 ps pulse width) as an excitation source. All fluorescence measurements were done using opaque films placed at 45° angle between the excitation source and the detector. Elemental composition of the quantum dot-sensitized films was determined by energy dispersive X-ray spectroscopy (EDS) using Hitachi S-4500 scanning electron microscopy.

Femtosecond Transient Absorption Spectroscopy. These measurements were conducted using a Clark MXR 2010 (775 nm, 1 mJ/pulse, fwhm pulse width = 130 fs, 1 kHz repetition) pump−probe laser system. 95% of the pump beam was directed though a second harmonic frequency doubler to produce 387 nm excitation wavelength used in all of the experiments. The remaining 5% of fundamental beam was passed through an optical delay stage for regulating the precise delay time between the pump and probe. The beam from the delay stage was passed though sapphire crystal to generate probe pulse of white light continuum, which was projected onto the sample. Spectral and temporal overlap of the pump and probe beams on the CdSe films held in a 0.2 cm path length quartz cuvette was achieved at an angle <10°. The probe beam was collected with a CCD spectrograph (Ocean Optics, S2000-UV−vis) providing a 450−800 nm data window. Typically, 1000 excitation pulses were averaged to obtain a transient spectrum at a set delay time.

For CdSe-sensitized films, it was observed that continuous exposure to high intensity pump beam during measurement caused degradation of the spot, as evidenced by both a decrease and red shift in the ground-state peak absorbance after laser exposure (see Discussion). The problem was more pronounced especially for films in pure Na_2S electrolyte. To overcome this, the experiments were done at relatively low intensity (13 mW/cm^2), and the measurements were done at four different spots on the sample surface. All kinetic traces shown are thus averaged data collected over different spots.

Nanosecond Flash Photolysis. Nanosecond absorption measurements were done with 532 nm excitation pump beam (pulse width = 10 ns, 10 Hz, and energy = 5 mJ) using a Nd:YAG laser from Spectra Physics (Quanta-Ray Pro230). The probe beam, which was at right angles to the pump beam, consisted of white light from a 1000 W xenon lamp (Hanovia) pulsed with a lamp pulser from Sorensen Power Supplies. The beam was collected using a monochromator (Digikrom 240, CVI Laser Corp.) and photomultiplier tube and was recorded using a computer interfaced 1 GHz LeCroy oscilloscope. The CdSe-sensitized films were placed in a 0.5 cm path length quartz cuvette held at 45° with respect to both pump and probe beams. Data sets reported herein typically were the signal average of five scans.

Photoelectrochemical Measurements. $I-V$ characteristics of the CdSe−TiO_2 films were measured using a two electrode setup with a platinum gauze as the counter electrode in a open cell configuration. The cell was continuously purged with N_2 throughout the measurement. Measurements were conducted using a Keithley 2601 programmable electrometer along with collimated, filtered light (λ > 420 nm) from a 300 W xenon arc lamp.

All spectroscopic and electrical characterization was done at room temperature in a freshly prepared 0.1 M Na_2S solution, which was degassed using N_2 before measurements.

RESULTS AND DISCUSSION

Hole Transfer from CdSe to Sulfide Redox Couple. The majority of studies to date have employed Na_2S as a regenerative electrolyte to maintain the stability of the CdSe film in the photoelectrochemical cell. It is important to note that the sulfide ions in aqueous medium predominantly exist as HS^- because of the equilibrium (1).

$$S^{2-} + H_2O \leftrightarrow HS^- + OH^- \quad (1)$$

Relatively high equilibrium constant produces OH^- and HS^- ions when Na_2S is dissolved in water.[30] The pH of a 0.1 M solution after dissolution of Na_2S is close to 13, indicating near complete shift of the equilibrium (1) to the right. Although the majority of the species exists as HS^-, we will refer to dissolved sulfide species as S^{2-} in the discussion below.

Upon bandgap excitation of the CdSe, the primary event is charge separation (reaction 2) followed by charge recombination and electron injection into the semiconductor oxide substrate (TiO_2). Thus, for CdSe/TiO_2 films subjected to bandgap excitation ($h\nu$), we expect charge carriers to undergo radiative

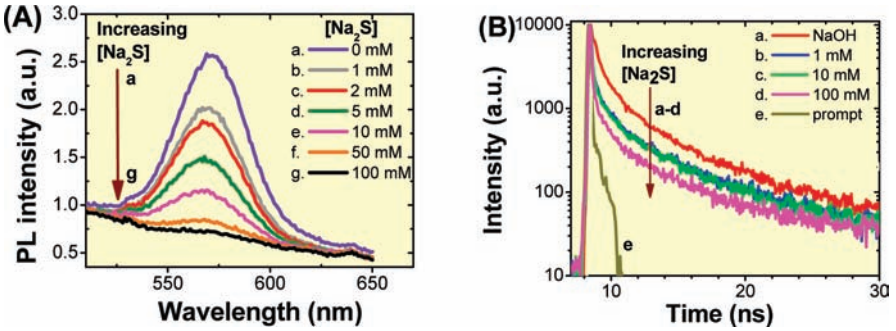

Figure 1. (A) Steady-state photoluminescence spectra of CdSe−SiO_2 film in contact with aqueous NaOH (pH = 13) solution containing (a) 0, (b) 1, (c) 2, (d) 5, (e) 10, (f) 50, (g) 100 mM of Na_2S. The emission spectra were recorded using 390 nm excitation. (B). Emission decay monitored at 580 nm of CdSe quantum dots anchored on SiO_2 film in contact with NaOH solution (pH = 13) containing (a) 0, (b) 1, (c) 10, (d) 100 mM Na_2S. Profile (e) corresponds to "prompt" instrument response measured against a blank SiO_2 film. The excitation wavelength was 373 nm.

recombination ($h\nu'$) or undergo charge separation by accumulating electrons in TiO_2 and holes in CdSe (reaction 3).

$$\mathrm{CdSe} + h\nu \rightarrow \mathrm{CdSe(h + e)} \rightarrow \mathrm{CdSe} + h\nu \qquad (2)$$

$$\mathrm{CdSe(h + e)} + \mathrm{TiO_2} \rightarrow \mathrm{CdSe(h)} + \mathrm{TiO_2(e)} \qquad (3)$$

$$\mathrm{CdSe(h)} + \mathrm{S^{2-}} \rightarrow \mathrm{CdSe} + \mathrm{S^{-\cdot}} \qquad (4)$$

Redox couples such as S^{2-}/S_n^{2-} are quite effective in scavenging the holes from CdSe (reaction 4). Because both electron and hole transfer contribute to the quenching of CdSe emission in CdSe/TiO_2 system, it is difficult to isolate these two processes from emission quenching measurements. On the other hand, a neutral oxide such as SiO_2 is a convenient substrate as it does not accept electrons from excited CdSe. Therefore, CdSe/SiO_2 films allowed us to monitor the emission quenching arising from hole transfer at the CdSe interface selectively. In the absence of Na_2S, the CdSe exhibits a natural decay as it undergoes charge recombination (reaction 2). In the presence of Na_2S, the hole transfer to S^{2-} competes with the charge recombination processes (reaction 4).

The emission spectra recorded in Figure 1A and the emission lifetime measurements (Figure 1B) show a decrease in the emission yield and emission lifetime, respectively. The lifetime traces were fitted to a triple exponential decay, resulting in long, medium, and fast lifetimes tabulated in Table S1.

The average lifetime (τ_0) of SiO_2/CdSe in 0.1 M NaOH corresponding to the natural radiative decay of CdSe quantum dots on SiO_2 surface was 4.58 ns. The lifetime decreased as the concentration of sulfide in solution was increased. An average emission lifetime (τ') of 3.3 ns was observed when CdSe/SiO_2 film was in contact with 0.1 M S^{2-} solution. If the decreased lifetime in S^{2-} is entirely due to the scavenging of holes (reaction 4), one can obtain the rate constant for electron transfer (k_{et}) from expression 5:

$$k_{et} = 1/\tau' - 1/\tau_0 \qquad (5)$$

The apparent rate constant obtained from the average lifetimes yields a value of 8.5×10^7 s^{-1} for the hole transfer to S^{2-}. It should be noted that this rate constant takes into account both fast and short lifetimes. If we consider the fast component alone, one could anticipate electron transfer rate constants as high as 7.33×10^9 s^{-1} in 0.1 M Na_2S solution. These values are lower in magnitude than the electron injection from excited CdSe into TiO_2 and other oxide semiconductors.[31,32] The size quantization effects of CdSe and density of states within the oxide substrate have also been shown recently to dictate the overall rate of the electron injection process.[33] However, because of the minimal movement in the valence band as a result of size quantization and relatively large energy difference between the valence band and sulfide redox couple, we do not expect to see an energy gap dependence of hole transfer rate constant. Emission quenching behavior was also monitored for CdSe−TiO_2 films in Na_2S solution (Figure S2 in the Supporting Information) where the changes in the luminescence decay of CdSe occur as a result of both electron transfer (to TiO_2) and hole transfer to S^{2-}/S_n^{2-} redox couple.

One can also argue whether the capping layer affects the hole transfer kinetics. Because the CdSe suspension was washed to remove excess TOPO layer, we consider such capping effects to be minimal. Furthermore, our previous studies with electron injection process have indicated that the interfacial electron transfer could occur with a rate constant as large as 10^{11} s^{-1}.[32,33] In addition, photoconversion efficiencies measured with and without capping layer in solar cells are comparable.

Femtosecond Transient Absorption Measurements. To probe the contribution of ultrafast events in the hole transfer process, we employed femtosecond transient spectroscopy. Figure 2A shows the time-resolved difference absorption spectra of CdSe−SiO_2 film in contact with Na_2S. Upon band gap excitation, CdSe quantum dots undergo charge separation as marked by the bleaching of the excitonic band at 560 nm. In the absence of any electron acceptor or donor molecules, the bleaching recovery reflects the disappearance of charge carriers via recombination and/or trapping at the defect states. If one of the charge carriers (electron or hole) is scavenged by an electron or hole acceptor molecule, the bleaching recovery becomes faster. Transient absorption measurements were recorded following 387 nm laser pulse excitation of CdSe−SiO_2 film in the presence and absence of Na_2S solution. The broad negative absorption peak seen at 560 nm is due to the ground-state bleach of $1S_{3/2}1S_e$ transition. For CdSe anchored on TiO_2, the injection of electrons into TiO_2 dominates the bleaching recovery process.[32] However, the bleaching recovery arising from hole transfer is usually small as reflected from the transient spectra in Figure 2.

Figure 2B shows the comparison of transient absorption kinetics of the CdSe−SiO_2 system monitored at 560 nm in NaOH and Na_2S electrolyte. In the presence of Na_2S in the

dx.doi.org/10.1021/ja203131b |J. Am. Chem. Soc. 2011, 133, 9607–9615

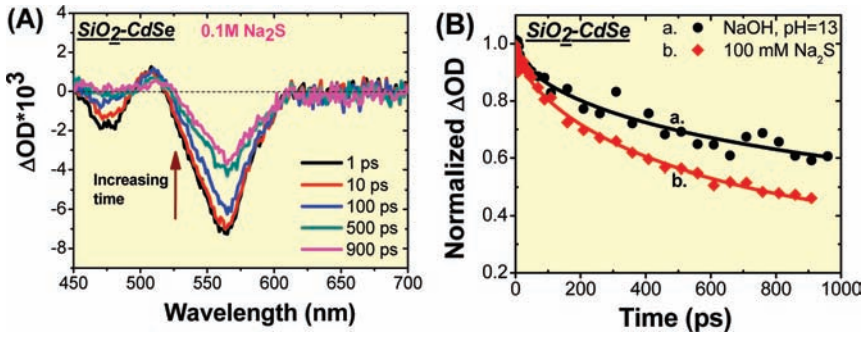

Figure 2. (A) Time-resolved transient absorption spectra of CdSe−SiO_2 film in contact with 0.1 M Na_2S electrolyte recorded following a 387 nm laser excitation. Arrow in the figure represents the bleaching recovery with increasing time. (B) Time-absorption profile at a probe wavelength of 560 nm recorded following the excitation of CdSe−SiO_2 film in (a) NaOH and (b) 100 mM Na_2S electrolyte. Solid lines are the kinetic fits obtained from the stretched exponential analysis.

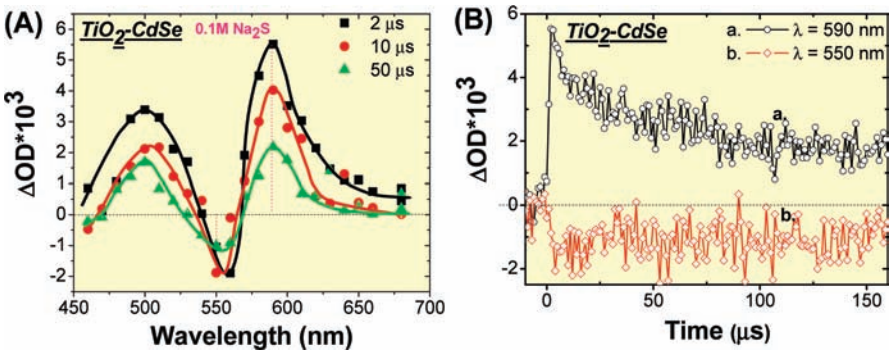

Figure 3. (A) Transient absorption spectra recorded at different time intervals after 532 nm laser pulse excitation (5 mJ/pulse, pulse width ~10 ns) of CdSe−TiO_2 film in 0.1 M Na_2S solution. (B) Transient absorption kinetics of CdSe−TiO_2 film in contact with 0.1 M Na_2S electrolyte recorded after 532 nm laser pulse excitation at probe wavelengths of 550 and 590 nm.

electrolyte, the bleaching recovery becomes slightly faster, but does not completely recover in the observable time scale (1.6 ns). The bleaching kinetics were fitted with a stretched exponential kinetics, and the fitting parameters are summarized in Table S2 in the Supporting Information. The average time constants for the initial part of bleaching recovery for CdSe−SiO_2 in contact with NaOH and Na_2S electrolytes were 1313 ± 96 and 645 ± 15 ps, respectively. As indicated in the emission lifetime decay measurements in the previous section, the hole scavenging by S^{2-} ions is relatively a slow process and occurs over a period of several nanoseconds.

Characterization of Hole Transfer Product in Sulfide Medium. It has been shown previously that the hole trapping as well as hole scavenging by S^{2-} produce $S^{-\cdot}$ radicals following the excitation of CdS or reaction with oxidizing radicals such as hydroxyl radicals.[34,35] If indeed the scavenging of the holes by S^{2-} at the CdSe interface produces $S^{-\cdot}$ radicals, we should be able to probe its formation through nanosecond transient absorption spectroscopy. Figure 3A shows the transient absorption spectra recorded following 532 nm laser pulse excitation of TiO_2−CdSe films immersed in 0.1 M Na_2S solution. As the photogenerated electrons are transferred to TiO_2, the holes accumulated within the CdSe are transferred to S^{2-}. The formation of $S^{-\cdot}$ is marked by a broad absorption in the visible 450−650 nm region. The split in the absorption band with a dip around 550 nm arises from the bleaching of the CdSe exciton band. This bleaching is likely to arise from the charging effects of surroundings (electrons in TiO_2 and $S^{-\cdot}$ at the interface) of the CdSe particle. As shown in a previous study, the broad absorption peak centered around λ = 590 nm can be assigned to the polysulfide radical.[36] As the photogenerated electrons are transferred to TiO_2 following charge separation, the holes accumulated within the CdSe are scavenged by the S^{2-} ions in the electrolyte to produce $S^{-\cdot}$ radical (reaction 4). The sulfide radical quickly complexes with S^{2-} ions and generate polysulfide radical. Because the exact chemical identity of polysulfide is difficult to establish, we will denote it by $(S_{n+1})^{-\cdot}$ (reaction 6).

$$S^{-\cdot} + nS^{2-} \rightarrow (S_{n+1})^{-\cdot} \quad (6)$$

Pulse radiolysis and other absorption measurements of polysulfide systems have established the absorption band of different intermediate species: $HS^{\cdot}$ (λ_{max} = 290−330 nm),[37] $S_2^{-\cdot}$ (λ_{max} = 400 nm),[38,39] $S_4^{-\cdot}$ (λ_{max} = 513 nm),[38,39] $H_2S_2^{-\cdot}$ (λ_{max} = 380 nm),[40] and $S_3^{-\cdot}$ (λ_{max} = 580−600 nm).[38,39] The broad absorption band seen in the transient absorption spectra suggests that two or more of these polysulfide species are formed as a result of the hole transfer process at the CdSe interface.

Although electrons injected into TiO_2 are also expected to give rise to a positive absorption in the 500−800 nm region,[41] we expect its contribution to be negligibly small.

Figure 3B shows transient absorption decays at 590 and 550 nm, which represent the decay of $S^{-\cdot}$ radical and bleaching recovery of CdSe, respectively. The $S^{-\cdot}$ radicals decays via recombination reaction with electrons that were injected into

dx.doi.org/10.1021/ja203131b | J. Am. Chem. Soc. 2011, 133, 9607–9615

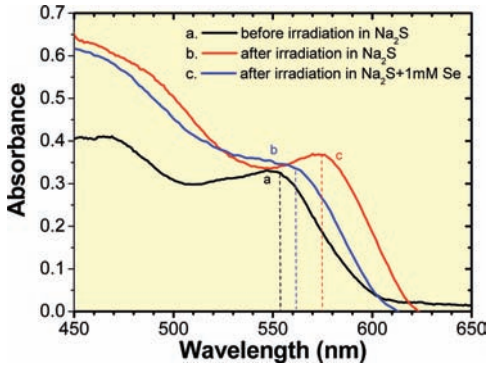

Figure 4. Diffuse reflectance spectra of CdSe−TiO_2 films (a) before and (b,c) after exposure to visible irradiation. The electrolyte contained (a,b) 0.1 M Na_2S and (c) 0.1 M Na_2S + 1.0 mM Se.

TiO_2 (reaction 7).

$$(S_{n+1})^{-\cdot} + TiO_2(e) \rightarrow (S_{n+1})^{2-} + TiO_2 \qquad (7)$$

From the transient decay at 590 nm, we obtain an average lifetime of 193 μs for $S^{-\cdot}$ radicals generated at the CdSe surface. The first-order rate constant derived from this lifetime yields a rate constant of 5.2 × 10^3 s^{-1} for the back electron transfer between electrons in the TiO_2 and $S^{-\cdot}$ radicals. This rate constant is at least 2 orders of magnitude greater than the one observed for $TiO_2(e)$ and I_3^- in the regeneration step of dye-sensitized solar cells.[42−44] The faster recombination seen in reaction 7 is one of the major hurdles that needs to be taken into account when designing quantum dot solar cells.

Any fraction of holes that escapes scavenging by the sulfide ions results in the formation of an oxidized product and Cd^{2+} at the surface (reaction 8).

$$2CdSe(h) \rightarrow CdSe + Cd^{2+} + Se^0 \qquad (8)$$

Cd^{2+} in turn can react with the S^{2-} to form a CdS layer on top of the CdSe (reaction 8):

$$Cd^{2+} + S^{2-} \rightarrow CdS \qquad (9)$$

Although the presence of S^{2-} in the electrolyte is expected to scavenge holes (reaction 4), the residual bleaching seen in the transient absorption trace at 550 nm (Figure 2B) shows irreversible changes, possibly arising from reactions 8 and 9. The steady-state absorption spectra, in Figure 4, of CdSe−TiO_2 electrodes after prolonged illumination in 0.1 M Na_2S showed both broadening and red shift of the excitonic peak. The spectra shifts were as large as 25 nm in many of these samples. This shift in absorption suggests that CdSe quantum dots undergo compositional changes and/or particle growth during photoirradiation in the presence of Na_2S electrolyte. Although CdSe quantum dots themselves show remarkable photostability, as evident from their use in solid-state solar cells, they undergo phototransformation when in contact with an aqueous sulfide solution.

The substituiton of the Se→S substitution reaction was also confirmed through EDS elemental analysis of the CdSe−TiO_2 electrodes (Figure S3A in the Supporting Information.) The sample after illumination of the TiO_2/CdSe film in Na_2S electrolyte shows a stronger S peak. On the basis of these observations, we can conclude that the photoanodic corrosion is responsible for the formation $CdSe_{1-x}S_x$ shell around the CdSe quantum dot. Scheme 2 illustrates the phototransformation of CdSe surface during irradiation in sulfide medium.

Scheme 2. Bandgap Excitation of TiO_2/CdSe Composite Resulting in the Formation of an Overcoat Layer of $CdSe_{1-x}S_x$

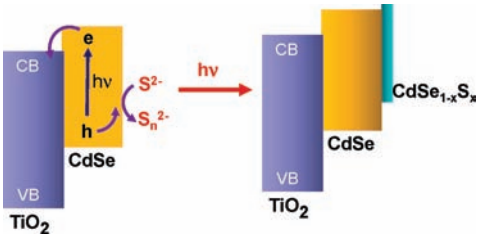

The presence of a medium band gap semiconductor such as $CdSe_{1-x}S_x$ on top of small band gap semiconductor (viz., CdSe) serves as an overcoat layer and thus prevents further corrosion. Because of the shift in the band edge to the red region, we can attribute the band energy of the overcoat layer to be smaller than that of parent CdSe. The red-shifted absorption also explains the mismatch between the absorption and excitation spectra in earlier published papers.[10,16,45] The quantum dot solar cells made from TiO_2/CdSe film continue to deliver stable photocurrent, which in turn indicates that the overcoat layer is not detrimental. In fact, an overcoat layer of metal sulfide (e.g., ZnS or CdS) is often used to improve the performance of CdSe or PbS quantum dot solar cells.[15,46] On the other hand, such an overcoat layer completely annihilates the photocurrent generation in the CdTe−TiO_2 system.[10]

Effect of S and Se on the Hole Scavenging Process. It has been shown earlier that sulfur dissolves in polysulfide solutions much faster than in an equimolar monosulfide solution as polysulfide is a stronger nucleophile than S^{2-} or HS^- ions in solution.[47] With this in mind, we investigated the effect of elemental sulfur and selenium on the hole scavenging rate of the S^{2-}/S_n^{2-} redox couple. Elemental S and Se complexes with Na_2S to yield an oxidized form of the redox couple, polysulfide and polyselenosulfide ions, respectively (see, for example, reaction 10).

$$nSe + S^{2-} \rightarrow (Se_nS)^{2-} \qquad (10)$$

Figures 5 shows nanosecond transient absorption spectra and the transient decay at 590 nm recorded following 532 nm laser pulse excitation of TiO_2/CdSe films immersed in 0.1 M Na_2S containing 5 mM Se. The presence of S or Se (viz., S_n^{2-} or $(S_{n+1}Se)^{2-}$) in the electrolyte is quite effective in maintaining the stability of the electrode. No residual bleaching is seen at 560 nm. The peak at 590 nm is similar to that seen for CdSe in pure Na_2S electrolyte (Figure 3A), which indicates that the absorption is a result of same charge transfer product, $S^{-\cdot}$ radical. A similar absorption peak was also seen for electrolyte containing polysulfide ions (see Figure S4 in the Supporting Information). In addition, the absorption spectra recorded with SiO_2/CdSe films (see Figure S5) also exhibited similar transient absorption features. The enhancement in the decay of $S^{-\cdot}$ represents increased rate of back electron transfer. Having greater concentration of polysulfide, the oxidized counterpart of the redox couple, renders the back electron transfer (reaction 7) to dominate.

dx.doi.org/10.1021/ja203131b |*J. Am. Chem. Soc.* 2011, 133, 9607–9615

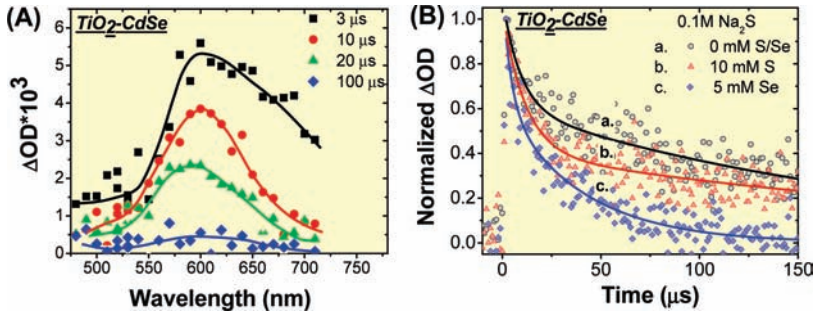

Figure 5. (A) Transient absorption spectra of CdSe−TiO_2 film in contact with 5 mM Se + 0.1 M Na_2S solution recorded after 532 nm laser pulse excitation. (B) Absorption time profiles of CdSe−TiO_2 film in contact with 0.1 M Na_2S containing (a) 0, (b) 10 mM S, and (c) 5 mM Se. Solid lines are the kinetic fits obtained from the biexponential analysis.

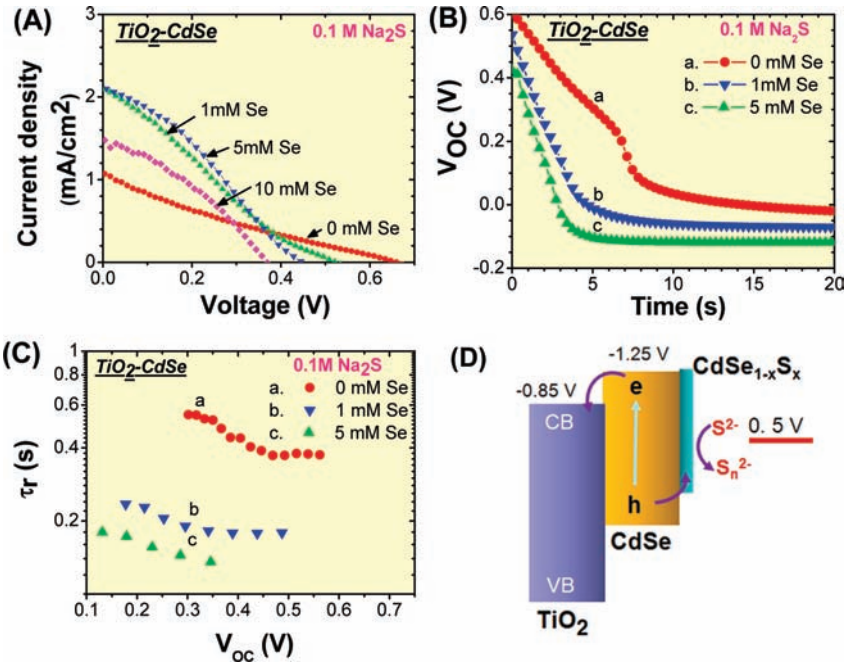

Figure 6. (A) $I-V$ characteristics of CdSe−TiO_2 electrodes in 0.1 M Na_2S electrolyte containing different concentrations of Se (excitation >420 nm; intensity 100 mW/cm^2). (B) Photovoltage decay response of CdSe−TiO_2 electrodes in Se containing Na_2S electrolyte after the white light illumination was turned off. (C). Back electron transfer time constant, τ_r, as estimated from the photovoltage decay curves for CdSe−TiO_2 in 0.1 M Na_2S electrolyte containing different concentration of Se. (D) Schematic diagram of TiO_2/CdSe/$CdSe_{1-x}S_x$ electrode in contact with S^{2-}/S_n^{2-} redox couple. The conduction band energies with respect to NHE refer to bulk TiO_2 and CdSe in contact with 0.1 M Na_2S (pH 13).[9]

The kinetics of the decay process was monitored at 590 nm and is shown in Figure 5B for Na_2S electrolytes containing S and Se. The absorption−time profiles representing the charge recombination were nonexponential and required fitting with at least two decay components. (See Table S3 in the Supporting Information for the amplitudes and the estimated average time constants of each components.) This nonexponential behavior is likely to arise from the complex nature of the S^{2-}/S_n^{2-} redox couple, which involves a complex equilibrium with several reactions occurring in parallel to the photoelectrochemical recombination reactions.

It should be noted that the presence of Se in the electrolyte assists in maintaining better stability than S^{2-} alone (see, for example, absorption changes in Figure 4). However, this beneficial role of Se comes with a penalty as it promotes back electron transfer process. Nearly 5 times enhancement in the back electron transfer rate is seen when 5 mM Se was added to the electrolyte ($k_{bet} = 2.4 \times 10^4\ s^{-1}$). Thus, during the operation of a quantum dot solar cell, this enhanced rate of back electron transfer impedes the performance of working electrode as it competes with the collection of the injected electrons at the TiO_2/CdSe interface. Hence, the efficiency of the solar cell would depend on the interplay between the forward hole transfer reaction and backward scavenging reactions.

EDS spectra of the photoelectrodes after continuous illumination in Na_2S electrolyte containing elemental Se showed only a weak S signal (Figure S3B in the Supporting Information). The presence of a $(Se_nS)^{2-}$ ion in the solution is thus beneficial as it protects the CdSe quantum dots better than does S_n^{2-} and minimizes the effects of photocorrosion. The UV−vis absorption measurements of Figure 4 further confirm this stability aspect of two electrolytes. The smaller shift in the excitonic peak of CdSe

dx.doi.org/10.1021/ja203131b |J. Am. Chem. Soc. 2011, 133, 9607–9615

Table 1. Effect of Redox Couple Composition on the Performance of QDSC

electrolyte	V_{OC} (V)	I_{SC} (mA/cm^2)	FF	η (%)
Na_2S	0.66	1.1	0.19	0.14
Na_2S + 1 mM Se	0.52	2.2	0.24	0.26
Na_2S + 5 mM Se	0.45	2.1	0.30	0.30
Na_2S + 10 mM Se	0.38	1.5	0.38	0.22

electrodes was observed after the visible irradiation of the electrode in contact with electrolyte containing dissolved Se as compared to pure Na_2S electrolyte.

Implication of Scavenging of Holes and Charge Recombination at the CdSe Interface in the Operation of QDSC. The electrodes employed in spectroscopic measurements were further evaluated for their photoelectrochemical performance. Because we employ open-cell configuration, the observed efficiencies are lower than the one obtained using sandwich cell configuration. Figure 6 shows the $I-V$ characteristics of TiO_2/CdSe electrode in aqueous Na_2S electrolyte containing different amounts of Se. The photoelectrochemical characteristics of the CdSe−TiO_2 electrode at different electrolyte compositions are summarized in Table 1.

In the absence of Se, we observe a relatively high open circuit potential of 0.66 V and a short circuit current of 1.1 mA/cm^2. The oxidation potential of the S^{2-}/S_n^{2-} redox couple decreases with increasing polysulfide or polysulfoselenide ions in the electrolyte. Because the open circuit voltage is dictated by the difference in the Fermi level of the working electrode (CdSe−TiO_2) and equilibrated redox potential at the counter electrode, an increase in the oxidized form of the redox couple (increase in Se concentration) results in lower open-circuit potential. This observed shift in V_{oc} is in agreement with the Nernstian behavior. Interestingly, we observe nearly doubling of the short circuit current when 1 and 5 mM Se were added to the electrolyte. The increase in oxidized form of the redox couple is expected to favor the discharge of electrons at the counter electrode. This aspect is also reflected in the improved fill factor of the QDSC. At very high concentrations of Se (>10 mM), we see a small drop in both photocurrent and photovoltage. Increased light absorption by the polysulfoselenide electrolyte and electron recombination with polysulfoselenide at the photoanode are expected to contribute adversely to the performance of the photoelectrochemical cell.

The presence of an oxidized counterpart, $(S_{1-x}Se_x)^{2-}$, also adversely affects the cell performance as it increases the electron recombination at the CdSe−TiO_2 electrode interface. Under illumination, the forward electron injection process (reaction 3), hole scavenging by the S^{2-} or $(S_{1-x}Se_x)^{2-}$ (reaction 4), and electron recombination (reaction 7) attain a steady state as reflected from the steady open-circuit potential. The excess electrons accumulated under open circuit condition dictates the apparent Fermi level of the photoanode and hence the open circuit potential. When the illumination is stopped, both reactions 3 and 4 cease, and the recombination of accumulated electrons with oxidized form of redox couple at the interface (reaction 7) dominates as evident from the decay of open circuit potential. The decay time constant of open-circuit potentials recorded after stopping the illumination is indicative of the susceptibility of the electrons accumulated in the CdSe−TiO_2 photoanode to charge recombination. Earlier studies have employed the open circuit potential decay after stopping the illumination of the photoanode to estimate the lifetime of the photoinjected electrons.[48−51] This approach allows the determination of the voltage-dependent time constant for the scavenging of photoelectrons, using the expression:

$$\tau_r = \frac{kT}{e}\left(\frac{dV_{OC}}{dt}\right)^{-1} \quad (11)$$

Figure 6B and C shows the photovoltage decay response and the estimated back electron transfer time constant for the CdSe−TiO_2 electrode immersed in Na_2S containing different concentrations of Se. The decreased electron lifetime with increasing concentration of Se (Figure 6C) confirms the ability of $(S_{n+1}Se)^{2-}$ to promote back electron transfer (reaction 7) at the semiconductor−electrolyte interface. Efforts have been made to suppress such charge recombination process by modifying the CdSe interface with TiO_2 and other chalcogenide layers.[46,52−57] Despite the changes in the open circuit voltage and scavenging rates, the overall efficiency of the solar cell more than doubled with the addition of selenium to the electrolyte.

As seen from the solar cell characteristics (Table 1), the presence of oxidized counterpart (S or Se) to the redox electrolyte exhibits an opposing influence on the performance of QDSC, while at low concentration it improves the photocurrent generation and increases the fill factor. However, at higher concentrations, the effects of charge recombination dominate and hence decrease the overall power conversion efficiency.

In the case of the dye-sensitized solar cell, the I_3^-/I^- redox couple works favorably as its contribution to back electron transfer is negligible because of its own interesting redox chemistry.[42,43] Meyer has recently highlighted the role of various electron transfer steps involved in the I−I bond formation.[44] Because of the corrosive properties of iodide on quantum dots, the I_3^-/I^- redox couple cannot be used in conjunction with CdSe QDSC. Sulfide/polysulfide redox couple has been the popular choice as the regenerative redox couple in these solar cells. Earlier studies have highlighted complexities influencing the energetics of the semiconductor as well as altering the semiconductor interface.[9,45,58−61]

CONCLUSION

Issues related to a regenerative redox couple have often been overlooked in recent literature of the QDSC. Most of these studies have focused on the design of photoanode to achieve higher photoconversion efficiencies. To construct a high efficiency QDSC, it is important to pay careful attention to the role of the redox couple. While quick scavenging of holes regenerates the sensitizer and prevents it from anodic corrosion, it also can contribute to the back electron transfer process. The kinetic measurements of hole transfer process reported in this study demonstrate relatively slower interfacial hole transfer kinetics of CdSe QDs as compared to electron injection into TiO_2. As a result of this slow regeneration step, the electrons accumulated within TiO_2 are susceptible for recombination at the interface, thus limiting the photocurrent generation efficiency. Surface modification of semiconductor quantum dots with a relay molecule or a barrier overcoat can provide new ways to suppress back electron transfer. In fact, deposition of thin TiO_2 layer has allowed the use of the I_3^-/I^- redox couple in a bilayer type QDSC.[54]

To date, the maximum reported power conversion efficiency of liquid junction solar cell based QDSC is in the range 3−4%.[62]

On the other hand, solid-state heterojunction-based solar cells have exhibited efficiencies in the range of 5%.[14,63,64] These efficiencies are significantly lower than the traditional dye-sensitized solar cells. However, between developing new materials for counter electrodes and controlling kinetics at the working electrode, there are ample opportunities for improving the QDSC.

■ ASSOCIATED CONTENT

Supporting Information. Experimental details, emission spectra of CdSe on silica, and emission lifetime analysis. This material is available free of charge via the Internet at http://pubs.acs.org.

■ AUTHOR INFORMATION

Corresponding Author

pkamat@nd.edu

Present Addresses

[‖]School of Chemical and Biomolecular Engineering, Georgia Institute of Technology, Atlanta, Georgia 30332, United States.

■ ACKNOWLEDGMENT

The research described herein was supported by the Office of Basic Energy Science of the Department of the Energy. V.C. also acknowledges the support of the ND Energy Center for providing the research fellowship. This is contribution NDRL-4887 from the Notre Dame Radiation Laboratory.

■ REFERENCES

(1) Kamat, P. V. *J. Phys. Chem. C* **2008**, *112*, 18737.
(2) Kamat, P. V.; Tvrdy, K.; Baker, D. R.; Radich, J. G. *Chem. Rev.* **2010**, *110*, 6664.
(3) Palomares, E.; Martinez-Ferrero, E.; Albero, J. *J. Phys. Chem. Lett.* **2010**, *1*, 3039.
(4) Mora-Sero, I.; Bisquert, J. *J. Phys. Chem. Lett.* **2010**, *1*, 3046.
(5) Ruhle, S.; Shalom, M.; Zaban, A. *ChemPhysChem* **2010**, *11*, 2290.
(6) Lando, D.; Manassen, J.; Hodes, G.; Cahen, D. *J. Am. Chem. Soc.* **1979**, *101*, 3969.
(7) Licht, S. *J. Phys. Chem.* **1986**, *90*, 1096.
(8) Licht, S.; Tenne, R.; Flaisher, H.; Manassen, J. *J. Electrochem. Soc.* **1986**, *133*, 52.
(9) Ellis, A. B.; Kaiser, S. W.; Bolts, J. M.; Wrighton, M. S. *J. Am. Chem. Soc.* **1977**, *99*, 2839.
(10) Bang, J. H.; Kamat, P. V. *ACS Nano* **2009**, *3*, 1467.
(11) Allongue, P.; Cachet, H.; Froment, M.; Tenne, R. *J. Electroanal. Chem. Interfacial Electrochem.* **1989**, *269*, 295.
(12) Trindade, T.; O'Brien, P.; Pickett, N. L. *Chem. Mater.* **2001**, *13*, 3843.
(13) Sheeney-Haj-Khia, L.; Basnar, B.; Willner, I. *Angew. Chem., Int. Ed.* **2005**, *44*, 78.
(14) Moon, S.-J.; Itzhaik, Y.; Yum, J.-H.; Zakeeruddin, S. M.; Hodes, G.; Gratzel, M. *J. Phys. Chem. Lett.* **2010**, *1*, 1524.
(15) Braga, A.; Gimenez, S.; Concina, I.; Vomiero, A.; Mora-Sero, I. *J. Phys. Chem. Lett.* **2011**, 454.
(16) Baker, D. R.; Kamat, P. V. *Adv. Funct. Mater.* **2009**, *19*, 805.
(17) Vogel, R.; Pohl, K.; Weller, H. *Chem. Phys. Lett.* **1990**, *174*, 241.
(18) Mora-Seró, I.; Giménez, S.; Moehl, T.; Fabregat-Santiago, F.; Lana-Villareal, T.; Gómez, R.; Bisquert, J. *Nanotechnol. Mesostruct. Mater.* **2008**, *19*, 424007.
(19) Guijarro, N.; Lana-Villarreal, T.; Mora-Sero, I.; Bisquert, J.; Gomez, R. *J. Phys. Chem. C* **2009**, *113*, 4208.
(20) Ham, D.; Mishra, K. K.; Rajeshwar, K. *J. Electrochem. Soc.* **1991**, *138*, 100.
(21) Yochelis, S.; Hodes, G. *Chem. Mater.* **2004**, *16*, 2740.
(22) Brown, P.; Kamat, P. V. *J. Am. Chem. Soc.* **2008**, *130*, 8890.
(23) Liu, L.; Hensel, J.; Fitzmorris, R. C.; Li, Y.; Zhang, J. Z. *J. Phys. Chem. Lett.* **2010**, *1*, 155.
(24) Watson, D. F. *J. Phys. Chem. Lett.* **2010**, *1*, 2299.
(25) Ellis, A. B.; Kaiser, S. W.; Wrighton, M. S. *J. Am. Chem. Soc.* **1976**, *98*, 1635.
(26) Ellis, A. B.; Kaiser, S. W.; Wrighton, M. S. *J. Am. Chem. Soc.* **1976**, *98*, 6855.
(27) Tenne, R.; Lando, D.; Mirovsky, Y.; Mueller, N.; Manassen, J.; Cahen, D.; Hodes, G. *J. Electroanal. Chem. Interfacial Electrochem.* **1983**, *143*, 103.
(28) Vainas, B.; Hodes, G.; Dubow, J. *J. Electroanal. Chem. Interfacial Electrochem.* **1981**, *130*, 391.
(29) Peng, Z. A.; Peng, X. *J. Am. Chem. Soc.* **2001**, *123*, 183.
(30) Steudel, R. . In *Elemental Sulfur and Sulfur-Rich Compounds II, Topics in Current Chemistry No. 231*; Steudel, R., Ed.; Springer: New York, 2003; Vol. II, 248 pages.
(31) Chakrapani, V.; Tvrdy, K.; Kamat, P. V. *J. Am. Chem. Soc.* **2010**, *132*, 1228.
(32) Robel, I.; Kuno, M.; Kamat, P. V. *J. Am. Chem. Soc.* **2007**, *129*, 4136.
(33) Tvrdy, K.; Frantszov, P.; Kamat, P. V. *Proc. Natl. Acad. Sci. U.S.A.* **2011**, *108*, 29.
(34) Kamat, P. V.; Ebbesen, T. W.; Dimitrijevic, N. M.; Nozik, A. J. *Chem. Phys. Lett.* **1989**, *157*, 384.
(35) Kamat, P. V.; Gopidas, K. R.; Dimitrijevic, N. M. *Mol. Cryst. Liq. Cryst.* **1990**, *183*, 439.
(36) Stroyuk, A. L.; Raevskaya, A. E.; Kuchmii, S. Y. *Theor. Exp. Chem.* **2004**, *40*, 130.
(37) Melnikov, M. Y.; Smirnov, V. A. *Handbook of Photochemistry of Organic Radicals: Absorption and Emission Properties, Mechanisms, Aging*; Begell House Publishers: Redding, CT, 1997.
(38) Chivers, T.; Drummond, I. *Inorg. Chem.* **1972**, *11*, 2525.
(39) Clark, R. J. H.; Cobbold, D. G. *Inorg. Chem.* **1978**, *17*, 3169.
(40) Mills, G.; Schmidt, K. H.; Matheson, M. S.; Meisel, D. *J. Phys. Chem.* **1987**, *91*, 1590.
(41) Tvrdy, K.; Kamat, P. V. *J. Phys. Chem. A* **2009**, *113*, 3765.
(42) Green, A. N. M.; Chandler, R. E.; Haque, S. A.; Nelson, J.; Durrant, J. R. *J. Phys. Chem. B* **2005**, *109*, 142.
(43) Peter, L. M. *J. Phys. Chem. C* **2007**, *111*, 6601.
(44) Meyer, G. J.; Rowley, J.; Farnum, B.; Ardo, S. Making and Breaking I−I Bonds for Solar Energy Conversion. *J. Phys. Chem. Lett.* **2010**, *1*, 3132−3140.
(45) Bang, J. H.; Kamat, P. V. *Adv. Funct. Mater.* **2010**, *20*, 1970.
(46) Shen, Q.; Kobayashi, J.; Diguna, L. J.; Toyoda, T. *J. Appl. Phys.* **2008**, *103*, 084304.
(47) Hartler, N.; Libert, J.; Teder, A. *Ind. Eng. Chem. Process Des. Dev.* **1967**, *6*, 398.
(48) Bisquert, J.; Zaban, A.; Salvador, P. *J. Phys. Chem. B* **2002**, *106*, 8774.
(49) Bisquert, J.; Fabregat-Santiago, F.; Mora-Sero, I.; Garcia-Belmonte, G.; Gimenez, S. *J. Phys. Chem. C* **2009**, *113*, 17278.
(50) Barea, E. M.; Shalom, M.; Giménez, S.; Hod, I.; Mora-Seró, I. n.; Zaban, A.; Bisquert, J. *J. Am. Chem. Soc.* **2010**, *132*, 6834.
(51) Baker, D. R.; Kamat, P. V. *J. Phys. Chem. C* **2009**, *113*, 17967.
(52) Niitsoo, O.; Sarkar, S. K.; Pejoux, C.; Ruhle, S.; Cahen, D.; Hodes, G. *J. Photochem. Photobiol., A* **2006**, *181*, 306.
(53) Sambur, J. B.; Parkinson, B. A. *J. Am. Chem. Soc.* **2010**, *132*, 2130.
(54) Shalom, M.; Albero, J.; Tachan, Z.; Martinez-Ferrero, E.; Zaban, A.; Palomares, E. *J. Phys. Chem. Lett.* **2010**, *1*, 1134.
(55) Diguna, L. J.; Shen, Q.; Kobayashi, J.; Toyoda, T. *Appl. Phys. Lett.* **2007**, *91*, 023116.
(56) Mora-Sero, I.; Gimenez, S.; Fabregat-Santiago, F.; Gomez, R.; Shen, Q.; Toyoda, T.; Bisquert, J. *Acc. Chem. Res.* **2009**, *42*, 1848.
(57) Berea, E. M.; Shalom, M.; Gimenez, S.; Hod, I.; Mora-Sero, I.; Zaban, A.; Bisquert, J. *J. Am. Chem. Soc.* **2010**, *132*, 6834.

(58) Hodes, G.; Miller, B. *J. Electrochem. Soc.* **1986**, *133*, 2177.
(59) Hodes, G. In *Energy Resources through Photochemistry and Catalysis*; Graetzel, M., Ed.; Academic: New York, 1983.
(60) Hodes, G.; Manassen, J.; Cahen, D. *J. Electrochem. Soc.* **1981**, *128*, 2325.
(61) Dobson, K. D.; Visoly-Fisher, I.; Hodes, G.; Cahen, D. *Adv. Mater.* **2001**, *13*, 1495.
(62) Gonzalez-Pedro, V.; Xu, X.; Mora-Sero, I.; Bisquert, J. *ACS Nano* **2010**, *4*, 5783.
(63) Chang, J. A.; Rhee, J. H.; Im, S. H.; Lee, Y. H.; Kim, H.-j.; Seok, S. I.; Nazeeruddin, M. K.; Gratzel, M. *Nano Lett.* **2010**, *10*, 2609.
(64) Pattantyus-Abraham, A. G.; Kramer, I. J.; Barkhouse, A. R.; Wang, X.; Konstantatos, G.; Debnath, R.; Levina, L.; Raabe, I.; Nazeeruddin, M. K.; Grätzel, M.; Sargent, E. H. *ACS Nano* **2010**, *4*, 3374.